LETTER

doi:10.1038/nature25007

RNA polymerase III limits longevity downstream of TORC1

Danny Filer[1], Maximillian A. Thompson[2], Vakil Takhaveev[3], Adam J. Dobson[1], Ilektra Kotronaki[1], James W. M. Green[2], Matthias Heinemann[3], Jennifer M. A. Tullet[2] & Nazif Alic[1]

Three distinct RNA polymerases transcribe different classes of genes in the eukaryotic nucleus[1]. RNA polymerase (Pol) III is the essential, evolutionarily conserved enzyme that generates short, non-coding RNAs, including tRNAs and 5S rRNA[2]. The historical focus on transcription of protein-coding genes has left the roles of Pol III in organismal physiology relatively unexplored. Target of rapamycin kinase complex 1 (TORC1) regulates Pol III activity, and is also an important determinant of longevity[3]. This raises the possibility that Pol III is involved in ageing. Here we show that Pol III limits lifespan downstream of TORC1. We find that a reduction in Pol III extends chronological lifespan in yeast and organismal lifespan in worms and flies. Inhibiting the activity of Pol III in the gut of adult worms or flies is sufficient to extend lifespan; in flies, longevity can be achieved by Pol III inhibition specifically in intestinal stem cells. The longevity phenotype is associated with amelioration of age-related gut pathology and functional decline, dampened protein synthesis and increased tolerance of proteostatic stress. Pol III acts on lifespan downstream of TORC1, and limiting Pol III activity in the adult gut achieves the full longevity benefit of systemic TORC1 inhibition. Hence, Pol III is a pivotal mediator of this key nutrient-signalling network for longevity; the growth-promoting anabolic activity of Pol III mediates the acceleration of ageing by TORC1. The evolutionary conservation of Pol III affirms its potential as a therapeutic target.

The task of carrying out transcription in the eukaryotic nucleus is divided among RNA Pol I, II and III[1,4]. This specialization is evident in the biogenesis of the translation machinery, a task that requires the co-ordinated activity of all three polymerases: Pol I generates the 45S pre-rRNA that is subsequently processed into mature rRNAs, Pol II transcribes various RNAs including mRNAs encoding ribosomal proteins, while Pol III provides the tRNAs and 5S rRNA. This costly process of generating protein synthetic capacity is tightly regulated to match the extrinsic conditions and the intrinsic need for protein synthesis by the key driver of cellular anabolism, TORC1[5,6]. The central position of TORC1 in the control of fundamental cellular processes is mirrored by the notable effect of its activity on organismal physiology: following its initial discovery in worms[7], inhibition of TORC1 has been demonstrated to extend lifespan in all tested organisms, from yeast to mice[8,9], with beneficial effects on a range of age-related diseases and dysfunctions[3,10]. TORC1 strongly activates Pol III transcription[5,6] and this relationship suggests the possibility that inhibition of Pol III promotes longevity.

In *Saccharomyces cerevisiae*, each of the 17 Pol III subunits is encoded by an essential gene. We generated a yeast strain in which the largest Pol III subunit (C160, encoded by *RPC160*, also known as *RPO31*)[4] is fused to the auxin-inducible degron (AID). The fusion protein can be targeted for degradation by the ectopically expressed E3 ubiquitin ligase (OsTir) in the presence of indole-3-acetic acid (IAA)[11] to achieve conditional inhibition of Pol III (Extended Data Fig. 1a). We confirmed that IAA treatment triggered degradation of the fusion protein (Fig. 1a), and observed that IAA treatment also improved the survival of the *RPC160–AID* strain upon prolonged culture (Fig. 1b). In addition, IAA treatment of the control strain lacking the AID fusion

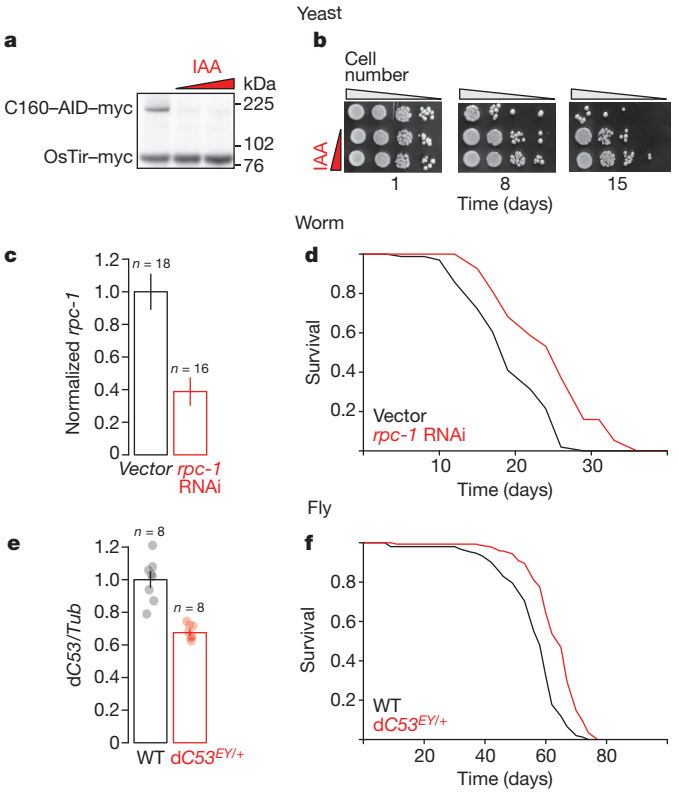

Figure 1 | Inhibition of Pol III extends lifespan. a, **b**, Treatment of the *RPC160-AID-myc pADH-OsTir-myc* budding yeast strain with 0, 0.125 and 0.25 mM IAA triggers degradation of C160–AID–myc (**a**) and extends its chronological lifespan (**b**), measured as colony formation after normalization for optical density and tenfold serial dilution (**a** and **b** show a representative of two experimental trials). **c**, **d**, Feeding *E. coli* expressing the *rpc-1* RNAi construct to N2 *C. elegans* from the L4 stage reduces the levels of *rpc-1* mRNA (**c**, $P < 10^{-4}$, two-tailed *t*-test) and extends the lifespan of worms relative to vector alone at 20 °C in the presence of 5′-fluorodeoxyuridine (FUDR) (**d**; log-rank test, $P = 0.03$; empty vector, $n = 86$; *rpc-1* RNAi, $n = 94$; representative of three trials). **e**, **f**, Female flies heterozygous for d$C53^{EY}$ have reduced d*C53* expression (**e**; two-tailed *t*-test, $P = 10^{-4}$; wild type (WT), 95% confidence intervals (c.i.) = 0.89–1.1; d$C53^{EY/+}$, c.i. = 0.64–0.71) and extended lifespan (**f**; log-rank test, $P = 6 \times 10^{-13}$; wild type, $n = 152$; d$C53^{EY/+}$, $n = 144$; single trial). Bar charts show mean ± s.e.m.; *n*, number of biologically independent samples; overlay, individual data points. For more detailed demography and a summary of worm and fly lifespan trials see Extended Data Figs 2c and 4a. Gel source data is shown in Supplementary Fig. 1.

[1]Institute of Healthy Ageing, Department of Genetics, Evolution and Environment, University College London, Gower Street, London WC1E 6BT, UK. [2]School of Biosciences, University of Kent, Canterbury CT2 7NJ, UK. [3]Molecular Systems Biology, Groningen Biomolecular Sciences and Biotechnology Institute, University of Groningen, 9747 AG Groningen, Netherlands.

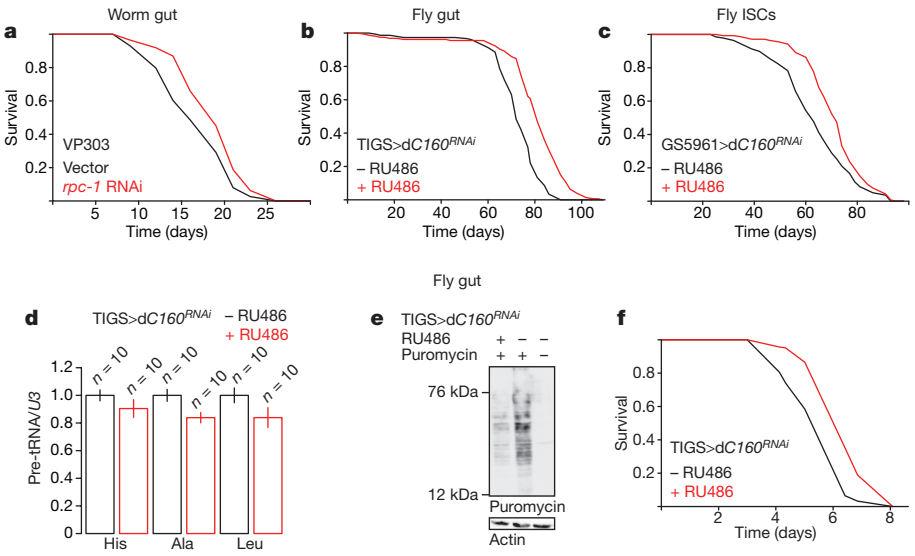

Figure 2 | Gut-specific inhibition of Pol III extends lifespan, reduces protein synthesis and increases tolerance to proteostatic stress. **a**, Induction of RNAi against *rpc-1* specifically in the worm gut by using the VP303 strain extends *C. elegans* lifespan at 20 °C in the presence of FUDR (log-rank test, $P = 0.02$; empty vector, $n = 90$; *rpc-1* RNAi, $n = 67$; representative of two trials). **b**, Feeding RU486 to female TIGS UAS-d*C160*^{RNAi} (TIGS > d*C160*^{RNAi}) flies to target d*C160* RNAi to the gut extends their lifespan (log-rank test, $P = 6 \times 10^{-16}$; no-RU486, $n = 150$; RU486, $n = 157$; representative of three trials). **c**, Feeding RU486 to female GS5961 > d*C160*^{RNAi} flies to target d*C160* RNAi to the ISCs extends their lifespan (log-rank test, $P = 2 \times 10^{-4}$; no RU486, $n = 139$; RU486, $n = 142$; representative of three trials). **d**–**f**, Inducing d*C160* RNAi expression in the gut by feeding RU486 to female TIGS > d*C160*^{RNAi} flies leads to: reduction in pre-tRNAs (**d**; bars, mean ± s.e.m.; multivariate analysis of variance (MANOVA), $P = 0.04$; $n = 10$ biologically independent samples per condition; left to right, c.i. = 0.91–1.1, 0.76–1.0, 0.90–1.1, 0.75–0.92, 0.88–1.1 and 0.68–1.0); reduction in gut protein synthesis, as quantified by *ex vivo* puromycin incorporation and western blotting (**e**; representative of three biologically independent repeats; see Extended Data Fig. 6c); and improved survival in response to tunicomycin challenge (**f**; log-rank test, $P = 3 \times 10^{-15}$; $n = 185$ animals per condition; representative of two trials). For more detailed demography and summary of lifespan trials see Extended Data Figs 2c and 4a. Gel source data is shown in Supplementary Fig. 1.

reduced its survival relative to both the same strain in the absence of IAA and to the *RPC160–AID* strain in the presence of IAA (Extended Data Fig. 1b). Hence, Pol III depletion appears to extend the chronological lifespan in yeast. While IAA had no substantial effect on the survival of a strain carrying the AID domain fused to the largest subunit of Pol II (*RPB220*, also known as *RP021*), this strain appeared to survive better than the control strain did in the presence of IAA (Extended Data Fig. 1a, b), indicating that inhibition of Pol II may also extend chronological lifespan. Chronological lifespan of yeast is a measure of survival in a nutritionally limited, quiescent population, whereas replicative lifespan measures the number of daughters produced by a single mother cell in its lifetime. We found no evidence that inhibition of Pol III causes an increase in the replicative lifespan in yeast (Extended Data Fig. 1c).

The observed increase in chronological lifespan may simply indicate increased stress resistance and hence be of limited relevance to organismal ageing. To examine the role of Pol III in organismal ageing directly, we turned to animal models. We initiated RNA-mediated interference (RNAi) against *rpc-1*, the *Caenorhabditis elegans* orthologue of *RPC160*, in worms from the L4 stage, causing a partial knockdown of *rpc-1* mRNA (Fig. 1c). This consistently extended the lifespan of worms at both 20 °C and 25 °C (Fig. 1d; Extended Data Fig. 2a–c). To reduce Pol III activity in *Drosophila melanogaster*, we back-crossed a P-element insertion that deletes the transcriptional start site of the gene encoding the Pol III-specific subunit C53 (*CG5147*^{EY22749}, henceforth called d*C53*^{EY}, Extended Data Fig. 3) into a healthy, outbred population of flies. Homozygous d*C53*$^{EY/EY}$ mutants were not viable, but heterozygous females had reduced d*C53* mRNA levels and lived longer than controls (Fig. 1e, f; Extended Data Fig. 4a). Taken together, our data strongly indicate that Pol III limits lifespan in multiple model organisms and conversely, that partial inhibition of its activity is an intervention that increases longevity in multiple species.

The longevity of an animal can be governed from a single organ. In the worm, this role is often played by the gut[12,13]. To restrict the *rpc-1* knockdown to the gut, we used worms deficient in *rde-1*, in which the RNAi machinery deficiency is restored in the gut by gut-specific *rde-1* rescue[14]. *rpc-1* RNAi extended the lifespan of this strain, both at 20 °C and 25 °C (Fig. 2a, Extended Data Fig. 2d). Similarly, in the adult fly, driving an RNAi construct targeting the *RPC160* orthologue (*CG17209*, henceforth called d*C160*, Extended Data Fig. 3) with the mid-gut-specific, RU486-inducible driver TIGS (ref. 15) extended the lifespan of females (Fig. 2b), while the presence of the inducer (RU486) did not affect survival of the control strains (Extended Data Fig. 4b, c). The longevity phenotype could also be recapitulated with RNAi against d*C53*, another Pol III subunit (Extended Data Fig. 4d), indicating that the phenotype was not subunit-specific or due to off-target effects. As well as the gut, longevity can also be associated with the fat body and neurons in flies[13]. However, the longevity phenotype caused by d*C160* RNAi appears to be specific to the gut, since no significant lifespan extension was observed upon induction of d*C160* RNAi in the fat body of the adult fly, and only a modest, albeit significant, extension resulted from neuronal induction of d*C160* RNAi (Extended Data Fig. 4e, f).

The worm gut is composed of only post-mitotic cells. In flies, as in mammals, the adult gut epithelium contains mitotically active intestinal stem cells[16] (ISCs). ISC homeostasis is important for longevity[17], and the mid-gut-specific driver TIGS appears to be active in at least some ISCs (Extended Data Fig. 5), prompting us to restrict d*C160* RNAi induction to this cell type. ISC-specific d*C160* RNAi, achieved with the GS5961 driver, was sufficient to promote longevity (Fig. 2c, see Extended Data Fig. 4b, g for controls). In summary, Pol III activity in the gut limits survival in worms and flies, and in the fly, Pol III can drive ageing specifically from the gut stem-cell compartment.

We assessed the consequences of Pol III inhibition in the fly gut. Pol III acts to generate precursor tRNAs (pre-tRNAs) that are processed rapidly to mature tRNAs. Owing to their short half-lives, pre-tRNAs are useful as readouts of *in vivo* Pol III activity. Profiling the levels of specific pre-tRNAs, pre-tRNA^{His}, pre-tRNA^{Ala} and pre-tRNA^{Leu}, relative to the levels of *U3* (a small nucleolar RNA transcribed by

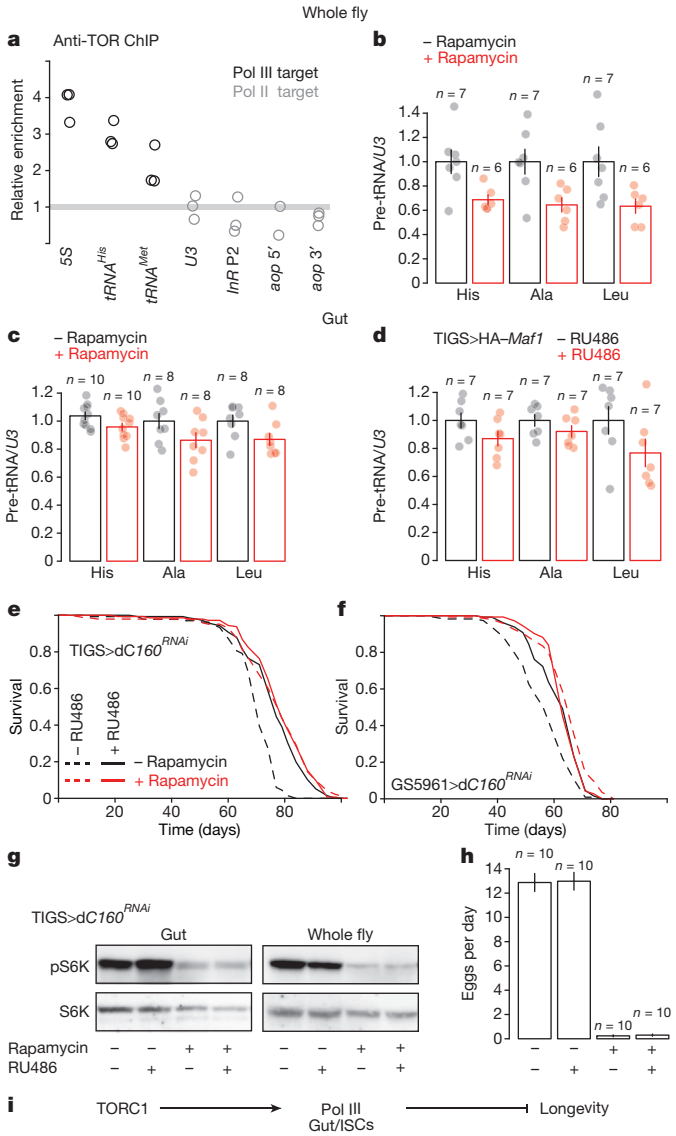

Figure 3 | Pol III regulates lifespan downstream of TORC1. a, ChIP against TOR shows higher relative enrichment of Pol III-transcribed genes compared to Pol II-transcribed genes (linear model with an a priori contrast, $P < 10^{-4}$; $n = 3$ biologically independent samples). **b**, **c**, Rapamycin feeding causes a decrease in pre-tRNAs relative to *U3* in whole female flies (**b**; MANOVA, $P = 0.01$; left to right, c.i. = 0.76–1.2, 0.58–0.79, 0.75–1.3, 0.49–0.79, 0.70–1.3 and 0.48–0.78); and their guts (**c**; MANOVA, $P = 0.01$; left to right, c.i. = 0.98–1.1, 0.90–1.0, 0.87–1.1, 0.74–0.99, 0.90–1.1 and 0.77–0.97). **d**, Induction of *Maf1* in the gut by feeding RU486 to female TIGS > HA–*Maf1* flies reduces the levels of pre-tRNAs relative to *U3* (MANOVA, $P = 4 \times 10^{-3}$; left to right, c.i. = 0.87–1.1, 0.74–1.0, 0.90–1.1, 0.82–1.0, 0.76–1.2 and 0.53–1.0). **e**, Induction of d*C160* RNAi in adult gut by feeding RU486 to female TIGS > d$C160^{RNAi}$ flies, and rapamycin feeding both extend lifespan, and their effects are not additive (Cox proportional hazards (CPH); rapamycin, $P = 2 \times 10^{-14}$; RU486, $P < 2 \times 10^{-16}$; interaction, $P = 7 \times 10^{-9}$; control, $n = 135$; RU486, $n = 144$; rapamycin, $n = 141$; RU486 + rapamycin, $n = 146$; single trial). **f**, Induction of d*C160* RNAi in ISCs by feeding RU486 to female GS5961 > d$C160^{RNAi}$ flies, and rapamycin feeding both extend lifespan and their effects are not additive (CPH; rapamycin, $P = 8 \times 10^{-14}$; RU486, $P = 2 \times 10^{-5}$; interaction, $P = 3 \times 10^{-7}$; control, $n = 113$; RU486, $n = 130$; rapamycin, $n = 145$; RU486 + rapamycin, $n = 144$; single trial). **g**, **h**, Treatment with rapamycin, but not d$C160^{RNAi}$ induction in the gut by feeding RU468 to female TIGS > d$C160^{RNAi}$ flies leads to a reduction in S6K phosphorylation in the gut and the whole fly (**g**; representative of four biologically independent repeats; see Extended Data Fig. 8c–f); and a reduction in egg laying (**h**; linear model; rapamycin, $P < 10^{-4}$; RU486, $P = 0.87$; interaction, $P = 0.96$). **i**, Model of the relationship linking TORC1, Pol III and lifespan. Bar charts show mean ± s.e.m.; *n*, number of biologically independent samples; overlay, individual data points. For more detailed demography, statistics and summary of lifespan trials see Extended Data Fig. 8a. Gel source data is shown in Supplementary Fig. 1.

Pol II[18]) revealed a moderate but significant reduction in Pol III activity upon gut-specific induction of d*C160* RNAi (Fig. 2d). The three polymerases can be directly coordinated to generate the translation machinery[19]. Indeed, Pol III inhibition had knock-on effects on Pol I- but not Pol II-generated transcripts, revealing partial cross-talk (Extended Data Fig. 6a, b). d*C160* RNAi also reduced protein synthesis in the gut (Fig. 2e, Extended Data Fig. 6c), consistent with reduced Pol III activity. These effects (reduction in pre-tRNAs or protein synthesis) were not observed after feeding RU486 to the driver-only control (Extended Data Fig. 6d–f). The reduction in protein synthesis was not pathological: total protein content of the gut was unaltered; fecundity, a sensitive readout of a female's nutritional status, was unaffected; and the flies' weight, triacylglycerol and protein levels remained unchanged (Extended Data Fig. 6g–i). Reduced protein synthesis can liberate protein-folding machinery from protein production and increase homeostatic capacity[20]. Indeed, induction of d*C160* RNAi in the gut increased the resistance of adult flies to proteostatic challenge with tunicamycin (Fig. 2f, and Extended Data Fig. 6j for TIGS-only control). Hence, Pol III can fine-tune the rate of protein synthesis in the adult fly gut without obvious detrimental outcomes, while increasing resistance to proteotoxic stress.

Having demonstrated the relevance of Pol III for ageing, we investigated whether it acts on lifespan downstream of TORC1 in *Drosophila*. Numerous observations in several organisms support the model in which TORC1 localizes on Pol III-transcribed loci and promotes phosphorylation of the components of the Pol III transcriptional machinery to activate transcription, in part by inhibition of the Pol III repressor, Maf1[5]. Using chromatin immunoprecipitation (ChIP) with two independently generated antibodies against *Drosophila* TOR (target of rapamycin)[21,22], we observed TOR enrichment on Pol III-target genes in the adult fly, relative to Pol II targets (Fig. 3a; Extended Data Fig. 7a–e). Inhibition of TORC1 by feeding rapamycin to flies reduced the levels of pre-tRNAs in whole flies (Fig. 3b). Rapamycin also reduced pre-tRNA levels specifically in the gut relative to *U3* (Fig. 3c). Since rapamycin results in re-scaling of the gut, evidenced by the reduction in the total RNA content of the organ (Extended Data Fig. 7f), we also confirmed that the drug reduced pre-tRNA levels relative to total RNA (Extended Data Fig. 7g). Interestingly, rapamycin did not cause a decrease in 45S pre-rRNA in the gut (Extended Data Fig. 7h, i), suggesting a lack of sustained Pol I inhibition. Additionally, gut-specific overexpression of *Maf1* reduced the levels of pre-tRNAs and extended lifespan (Fig. 3d, Extended Data Fig. 7j), confirming that Maf1 acts on Pol III in the adult gut. These data are consistent with TORC1 driving systemic and gut-specific Pol III activity in the adult fruitfly.

To examine whether the lifespan effects of Pol III are downstream of TORC1, we combined adult-onset Pol III inhibition with rapamycin treatment. Rapamycin feeding or gut-specific d*C160* RNAi resulted in the same magnitude of lifespan extension (Fig. 3e). The two treatments were not additive (Extended Data Fig. 8a), consistent with their acting on the same longevity pathway. The same effect was observed with RNAi against d*C53* in the gut (Extended Data Fig. 8b), as well as when d*C160* RNAi was restricted to the ISCs (Fig. 3f). Importantly, rapamycin feeding also inhibited phosphorylation of the TORC1 substrate, S6 kinase[3] (S6K), in both the gut and the whole fly, and decreased fecundity, while gut-specific *C160* RNAi did not have these effects (Fig. 3g, h, Extended Data Fig. 8c–f). This confirms that Pol III inhibition does not impact TORC1 activity locally or systemically, and therefore, Pol III acts downstream of TORC1 in ageing (Fig. 3i).

TORC1 inhibition is known to ameliorate age-related pathology and functional decline of the gut[23]. We examined whether inhibition of Pol III was sufficient to block the dysplasia resulting from

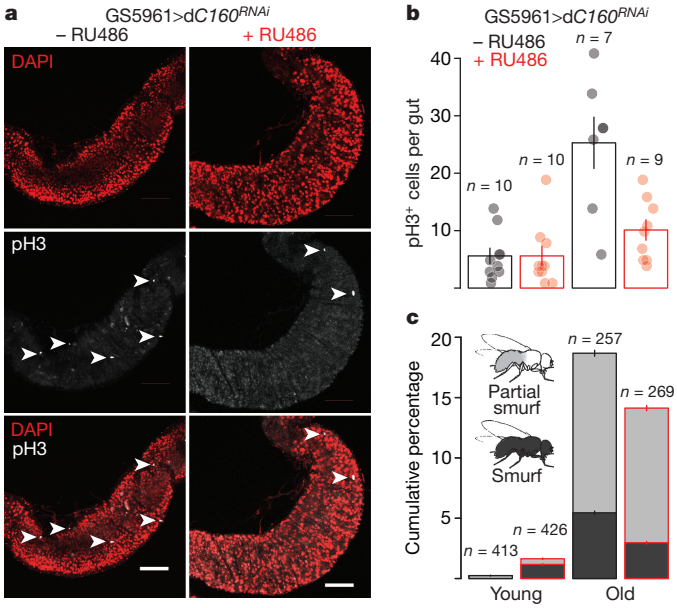

Figure 4 | Stem-cell-restricted Pol III inhibition improves age-related dysplasia and gut barrier function. a, **b**, d*C160* RNAi induction in ISCs by feeding RU486 to adult female GS5961 > d$C160^{RNAi}$ flies suppresses age-related accumulation of pH3-positive ($pH3^+$) cells: images of pH3 staining in the posterior mid-gut at 70 days of age (**a**; scale bars, 100 μm; arrows, pH3-positive cells; representative of nine RU486-fed animals and seven negative controls); the number of pH3-positive cells per gut (**b**; linear model; age, $P < 10^{-4}$; RU486, $P = 2 \times 10^{-3}$; interaction, $P = 2 \times 10^{-3}$; young, 7–9 days; old, 56–70 days; left to right, c.i. = 2.6–8.6, 1.8–9.4, 14–36 and 6.0–14). **c**, d*C160* RNAi induction in ISCs by feeding RU486 to adult female GS5961 > d$C160^{RNAi}$ flies reduces the age-related increase in the number of flies with a leaky gut (ordinal logistic regression (OLR); age, $P < 10^{-4}$; RU486, $P = 0.09$; interaction, $P = 0.01$; young, 21 days; old, 58 days; left to right, c.i. = 0.19–0.28, 1.5–1.8, 18–19 and 14–15 percentage of Smurfs). Bar charts, mean ± s.e.m.; *n*, number of animals; overlay, individual data points.

hyperproliferation and aberrant differentiation of ISCs by assessing the characteristic, age-dependent increase in dividing phospho-histone H3 (pH3)-positive cells[17]. Inducing d*C160* RNAi in the fly gut or solely in the ISCs ameliorated this pathology (Fig. 4a, b, Extended Data Fig. 9a). These treatments also counteracted the age-related loss of gut barrier function, decreasing the number of flies displaying extra-intestinal accumulation of a blue food dye (the 'Smurf' phenotype[24], Fig. 4c, Extended Data Fig. 9b). We also found that *rpc-1* RNAi reduced the severity of age-related loss of gut-barrier function in worms (Extended Data Fig. 9c). In *Drosophila*, gut health[25] and TORC1 inhibition[26] are specifically linked to female survival. Indeed, induction of d*C160* RNAi in the gut had a sexually dimorphic effect on lifespan, as the effect on males, although significant, was lower in magnitude relative to the effect on females (Extended Data Fig. 9d). Overall, our data show that gut- or ISC-specific inhibition of Pol III, which extends lifespan, is sufficient to ameliorate age-related impairments in gut health, which may be causative of or correlate with this longevity.

Our study demonstrates that the adult-onset decrease in the growth-promoting anabolic function mediated by Pol III in the gut, and specifically in the intestinal stem-cell compartment, is sufficient to recapitulate the longevity benefits of rapamycin treatment. Pol III activity is essential for growth[6]; its detrimental effects on ageing suggest an antagonistic pleiotropy[27] in which wild-type levels of Pol III activity are optimised for growth and reproductive fitness in early life but prove detrimental for later health. We reveal a fundamental role for Pol III in adult physiology, implicating wild-type Pol III activity in age-related stem-cell dysfunction, declining gut health and organismal survival downstream of nutrient signalling pathways. The longevity resulting from partial Pol III inhibition in adulthood is likely to result from the reduced provision of protein synthetic machinery; however, differential regulation of tRNA genes or Pol III-mediated changes to chromatin organization may also be involved, as has been suggested in other contexts[2]. The strong structural and functional conservation of Pol III in eukaryotes suggests that studies of its influence on mammalian ageing are warranted and could lead to important therapies.

Online Content Methods, along with any additional Extended Data display items and Source Data, are available in the online version of the paper; references unique to these sections appear only in the online paper.

Received 5 October 2016; accepted 7 November 2017.
Published online 29 November 2017.

1. Roeder, R. G. & Rutter, W. J. Multiple forms of DNA-dependent RNA polymerase in eukaryotic organisms. *Nature* **224,** 234–237 (1969).
2. Arimbasseri, A. G. & Maraia, R. J. RNA polymerase III advances: structural and tRNA functional views. *Trends Biochem. Sci.* **41,** 546–559 (2016).
3. Kennedy, B. K. & Lamming, D. W. The mechanistic target of rapamycin: the grand conducTOR of metabolism and aging. *Cell Metab.* **23,** 990–1003 (2016).
4. Vannini, A. & Cramer, P. Conservation between the RNA polymerase I, II, and III transcription initiation machineries. *Mol. Cell* **45,** 439–446 (2012).
5. Moir, R. D. & Willis, I. M. Regulation of pol III transcription by nutrient and stress signaling pathways. *Biochim. Biophys. Acta* **1829,** 361–375 (2013).
6. Grewal, S. S. Why should cancer biologists care about tRNAs? tRNA synthesis, mRNA translation and the control of growth. *Biochim. Biophys. Acta* **1849,** 898–907 (2015).
7. Vellai, T. *et al.* Genetics: influence of TOR kinase on lifespan in *C. elegans*. *Nature* **426,** 620 (2003).
8. Powers, R. W. III, Kaeberlein, M., Caldwell, S. D., Kennedy, B. K. & Fields, S. Extension of chronological life span in yeast by decreased TOR pathway signaling. *Genes Dev.* **20,** 174–184 (2006).
9. Harrison, D. E. *et al.* Rapamycin fed late in life extends lifespan in genetically heterogeneous mice. *Nature* **460,** 392–395 (2009).
10. Bitto, A. *et al.* Transient rapamycin treatment can increase lifespan and healthspan in middle-aged mice. *eLife* **5,** e16351 (2016).
11. Nishimura, K., Fukagawa, T., Takisawa, H., Kakimoto, T. & Kanemaki, M. An auxin-based degron system for the rapid depletion of proteins in nonplant cells. *Nature Methods* **6,** 917–922 (2009).
12. Libina, N., Berman, J. R. & Kenyon, C. Tissue-specific activities of *C. elegans* DAF-16 in the regulation of lifespan. *Cell* **115,** 489–502 (2003).
13. Piper, M. D., Selman, C., McElwee, J. J. & Partridge, L. Separating cause from effect: how does insulin/IGF signalling control lifespan in worms, flies and mice? *J. Intern. Med.* **263,** 179–191 (2008).
14. Espelt, M. V., Estevez, A. Y., Yin, X. & Strange, K. Oscillatory Ca^{2+} signaling in the isolated *Caenorhabditis elegans* intestine: role of the inositol-1,4,5-trisphosphate receptor and phospholipases C β and γ. *J. Gen. Physiol.* **126,** 379–392 (2005).
15. Poirier, L., Shane, A., Zheng, J. & Seroude, L. Characterization of the *Drosophila* gene-switch system in aging studies: a cautionary tale. *Aging Cell* **7,** 758–770 (2008).
16. Lemaitre, B. & Miguel-Aliaga, I. The digestive tract of *Drosophila melanogaster*. *Annu. Rev. Genet.* **47,** 377–404 (2013).
17. Biteau, B. *et al.* Lifespan extension by preserving proliferative homeostasis in *Drosophila*. *PLoS Genet.* **6,** e1001159 (2010).
18. Dieci, G., Preti, M. & Montanini, B. Eukaryotic snoRNAs: a paradigm for gene expression flexibility. *Genomics* **94,** 83–88 (2009).
19. Laferte, A. *et al.* The transcriptional activity of RNA polymerase I is a key determinant for the level of all ribosome components. *Genes Dev.* **20,** 2030–2040 (2006).
20. Harding, H. P., Zhang, Y., Bertolotti, A., Zeng, H. & Ron, D. Perk is essential for translational regulation and cell survival during the unfolded protein response. *Mol. Cell* **5,** 897–904 (2000).
21. Nagy, P. *et al.* Atg17/FIP200 localizes to perilysosomal Ref(2)P aggregates and promotes autophagy by activation of Atg1 in *Drosophila*. *Autophagy* **10,** 453–467 (2014).
22. Tsokanos, F. F. *et al.* eIF4A inactivates TORC1 in response to amino acid starvation. *EMBO J.* **35,** 1058–1076 (2016).
23. Fan, X. *et al.* Rapamycin preserves gut homeostasis during *Drosophila* aging. *Oncotarget* **6,** 35274–35283 (2015).
24. Rera, M., Clark, R. I. & Walker, D. W. Intestinal barrier dysfunction links metabolic and inflammatory markers of aging to death in *Drosophila*. *Proc. Natl Acad. Sci. USA* **109,** 21528–21533.
25. Regan, J. C. *et al.* Sex difference in pathology of the ageing gut mediates the greater response of female lifespan to dietary restriction. *eLife* **5,** e10956 (2016).
26. Bjedov, I. *et al.* Mechanisms of life span extension by rapamycin in the fruit fly *Drosophila melanogaster*. *Cell Metab.* **11,** 35–46 (2010).
27. Williams, G. C. Pleiotropy, natural-selection, and the evolution of senescence. *Evolution* **11,** 398–411 (1957).

Supplementary Information is available in the online version of the paper.

Acknowledgements The authors thank S. Grewal, B. Ohlstein, L. Partridge and S. Pletcher for fly lines; C. Bouchoux and F. Uhlmann for yeast reagents; G. Juhasz and A. Teleman for antibodies; E. Bolukbasi and L. Partridge for the Flag-tagged *d*Tor construct and S2 cells; M. Hill and D. Ivanov for help with RNA-seq analysis; L. Conder, A. Garaeva, D. Mostapha, G. Phillips and P. van der Poel for technical assistance, and M. Piper, J. Bähler and the IHA members for support, comments and critical reading of the manuscript. Reagents were obtained from Developmental Studies Hybridoma Bank, Vienna *Drosophila* Resource Centre, Bloomington Stock Center and the CGC, which is funded by NIH Office of Research Infrastructure Programs (P40 OD010440). This work was funded in part by Biotechnology and Biological Sciences Research Council grant BB/M029093/1, Royal Society grant RG140694 and Medical Research Council grant MR/L018802/1 to N.A., and Royal Society grant RG140122 to J.M.A.T. M.H. and V.T. received funding from the European Union's Horizon 2020 research and innovation programme under the Marie Sklodowska-Curie grant agreement 642738. D.F. is a recipient of the UCL Impact PhD studentship.

Author Contributions N.A. conceived the study; D.F. and N.A. made the yeast strains and performed chronological lifespan experiments; V.T. performed and analysed yeast replicative lifespan experiments under the supervision of M.H.; M.A.T. and J.W.M.G. performed and analysed worm experiments under the supervision of J.M.A.T.; D.F., A.J.D., I.K. and N.A. performed and analysed fly experiments under the supervision of N.A.; D.F., M.A.T., J.M.A.T. and N.A. wrote the manuscript with contributions from A.J.D.

Author Information Reprints and permissions information is available at www.nature.com/reprints. The authors declare no competing financial interests. Readers are welcome to comment on the online version of the paper. Publisher's note: Springer Nature remains neutral with regard to jurisdictional claims in published maps and institutional affiliations. Correspondence and requests for materials should be addressed to N.A. (n.alic@ucl.ac.uk) or J.M.A.T. (j.m.a.tullet@kent.ac.uk).

Reviewer Information *Nature* thanks N. Blewett, R. Maraia and the other anonymous reviewer(s) for their contribution to the peer review of this work.

METHODS

No statistical methods were used to predetermine sample size. Where animals of the same genotype were assigned to different treatments, the assignment was done randomly and in a way to avoid batching effects; no other randomization procedures were used. The investigators were not blinded to allocation during experiments and outcome assessment.

Yeast stocks, chronological lifespans and microfluidics assessment. A pMK43-based cassette was integrated into w303 *MATa leu2-3,112 trp1-1 can1-100 ura3-1 pADH-OsTir-9Myc::ADE2::ade2-1 his3-11,15* to produce RPC160 or RPB220 C-terminal AID fusions as previously described[11]. Strains were confirmed by PCR and absence of growth in presence of 2.5 mM IAA. The following primers were used for strain construction: *C160* forward, TGTCTATTTGAAAGTCTCTCAAATGAGGCAGCTTTAAAAGCGAACCGTACGCTGCAGGTCGAC; *C160* reverse, AGAAAAATAATACAAATGCTATAAAAAAGTTTAAAAACGACTACTATCGATGAATTCGAGCTCG; *B220* forward, CCAAAGCAAGACGAACAAAAGCATAATGAAAATGAAAATTCCAGACGTACGCTGCAGGTCGAC; *B220* reverse, ATATATAATGTAATAACGTCAAATACGTAAGGATGATATACTATAATCGATGAATTCGAGCTCG. The following primers were used for verification: *C160* forward, TTGGGTCAAACGATGTCG; B220 forward, CGCCTTCATACTCTCCAAC; *C160*/*B220* reverse, TGCCCATCATGGTACCTG.

For chronological lifespan experiments, the strains were grown to exponential phase ($OD_{600\,nm} \approx 0.4$) in Synthetic Complete medium (2% glucose, 0.5% ammonium sulfate, 0.17% yeast nitrogen base, 0.001% each of adenine, uracil, tryptophan, histidine, arginine and methionine, 0.0025% phenylalanine, 0.003% each of tyrosine and lysine, 0.004% isoleucine, 0.005% each of glutamate and aspartate, 0.0075% valine, 0.01% threonine, 0.02% each of serine and leucine (w/v)), the culture was split and treated with IAA in acetone or acetone alone (0.1%, day 0) and incubated with aeration and shaking at 30 °C. Samples were collected for protein extraction after 30 min. The cultures essentially reached stationary phase after 24 h. Viability was measured on the indicated days by plating 5 µl of tenfold serial dilutions, starting from an initial concentration corresponding to $OD_{600\,nm} = 0.5$, on YEPD plates and growing them for 2 days at 30 °C.

For replicative lifespan experiments, cells from single colonies were inoculated in 10 ml of minimal medium[28] containing 1% glucose, 0.02% leucine and 0.001% each of tryptophan, arginine, histidine and uracil (w/v) (pH 5, maintained with potassium phthalate–KOH buffer). The cultures were cultivated overnight in 100 ml flasks at 30 °C, shaking at 300 r.p.m. The following morning, cultures were diluted to an $OD_{600\,nm}$ of 0.005–0.01 while still in the exponential growth phase, and cultivated for several hours to an $OD_{600\,nm}$ of 0.045–0.09. They were then loaded into the microfluidics device as previously described[29,30], the growth medium having been aerated in advance by shaking for at least 2 h. Cells in the device were constantly supplied with fresh medium containing the synthetic auxin hormone 1-naphthaleneacetic acid (NAA) at concentrations of 0.0005, 0.001, 0.005 or 0.01 mM; the control medium did not contain NAA. These concentrations of the hormone span the dynamic range of the auxin-based degron system with which the degree of protein depletion can be efficiently modulated in this setup[31]. The temperature was maintained at 30 °C throughout the experiment.

Bright-field images were recorded at 5-min intervals for up to 5 days, using a Nikon Ti-E inverted microscope equipped with a 40× Nikon Super Fluor Apochromat objective and a halogen lamp with an additional UV-blocking filter. Time points of budding events, the eventual cell losses due to wash away or cell death were recorded by visual inspection of the time-lapse images with the help of ImageJ and a custom macro. For assessment of cell division times, the first six cell cycles of each cell were used.

Worm husbandry, lifespans and gut integrity assay. Before experiments, animals were maintained at 20 °C and grown for at least three generations with ample OP50 *E. coli* food to assure full viability. Hermaphrodites were used for experiments. The *rpc-1* RNAi clone (gene code C42D4.8) was obtained from the Ahringer *C. elegans* RNAi library. Lifespan assays were performed on HT115 *E. coli* expressing either the *rpc-1* RNAi plasmid or the pL4440 empty vector control as food source. Experiments were carried out at both 20 °C and 25 °C. Worms were scored as dead or alive at intervals, and worms that crawled off the plate, died from explosion or displayed bagging phenotypes were censored. *rpc-1* RNAi treatment from the L4 stage increased the incidence of a vulval-explosion phenotype (noted in Extended Data Fig. 2c). However, we found that this phenotype was greatly reduced at 25 °C (Extended Data Fig. 2c). The VP303 strain[14] was used for gut-targeted RNAi experiments. The Smurf assay for gut integrity was carried out essentially as previously described[32]. Worms were aged from the L4 stage at 25 °C and soaked in blue dye for 3 h at the desired age. The dye was removed by allowing the worms to move around on a bacterial lawn for 30 min before microscopy analysis. Individual worms were scored on their degree of 'Smurfness', with 0 signifying no blue beyond the gut barrier and 4 signifying complete dispersion of blue dye.

Fly husbandry, lifespan, tunicamycin survival, Smurf and fecundity assays. The outbred wild-type stock was collected in 1970 in Dahomey (now Benin) and has been kept in population cages to maintain lifespan and fecundity at levels similar to wild-caught flies. The w^{1118} mutation was backcrossed into the stock and *Wolbachia* was cleared by tetracycline treatment. TIGS (ref. 15, also known as TIGS-2), GS5961[33], S_1106[34], elavGS[35], UAS–HA–Maf1[36], UAS–dC160^{RNAi} and UAS-dC53^{RNAi} (v30512 and v103810 from Vienna *Drosophila* Resource Centre), and dC53^{EY22749} (CG5147^{EY22749} from Bloomington Stock Centre) were all backcrossed at least 6 times into the w^{1118} Dahomey background.

Stocks were maintained and experiments were conducted at 25 °C on a 12 h light:12 h dark cycle at 60% humidity, on SYA food[37] containing 10% brewer's yeast, 5% sucrose, and 1.5% agar (all w/v, with propionic acid and Nipagin as preservatives). RU486 (Sigma) and rapamycin (LC Laboratories, both dissolved in ethanol) were added to a final concentration of 200 µM as required. Tunicamycin (10 mg l^{-1}, Cell Signaling, DMSO stock) was added to sugar and agar food. In control treatments, equivalent volumes of the vehicle alone were added.

Flies were reared at standardized larval density and adults were collected over 12 h, allowed to mate for 48 h and sorted into experimental vials at a density of 15 flies per vial (10 flies per vial for RNA extractions). For lifespan experiments, flies were transferred to fresh vials and their survival was scored three times a week. Flies were transferred onto food containing tunicamycin on day 9 and survival was scored once or twice daily. For Smurf assays, flies at the indicated age were placed on SYA food containing 2.5% (w/v) blue dye (FD & C blue dye no. 1, Fastcolors) for 48 h. Flies were scored as full Smurfs if completely blue and partial Smurfs if the dye had leaked out of the gut but had not reached the head. Eggs laid over ~24 h were counted on day 10. Other phenotypic tests were performed essentially as previously described[38].

RNA extraction, qPCR and RNA sequencing. Synchronised populations of worms were grown at 20 °C on control or *rpc-1* RNAi-containing substrate at the L4 stage, and collected after 4 days. Ten whole adult flies, or ten dissected mid-guts, were harvested on day 7–9. Total RNA was isolated using TRIZOL (Invitrogen). RNA isolation was quantitative—the amount obtained was proportional to the starting amount. RNA was converted to cDNA using random hexamers and Superscript II (Invitrogen). Quantitative PCR was performed using Power SYBR Green PCR Master Mix (ABI), using the relative standard curve method. For worms, *rpc-1* transcript levels were normalized to the geometric mean of three stably expressed reference genes: *cdc-42*, *pmp-3* and *Y45F10D.4* as previously described[39]. For fly experiments, the following primers specific for pre-tRNAs were designed based on previous biochemical characterization[40] or predicted intronic sequences[41]: d*C53* (CG5147) forward, GGGTGACCCAGAGTCCCT; d*C53* (CG5147) reverse, GGCGAGCTCAGCGAAGAG; pre-rRNA ITS forward, TTAGTGTGGGGCTTGGCAACCT; pre-rRNA ITS reverse, CGCCGTTGTTGTAAGTACTCGCC; pre-rRNA ETS forward, GTTGCCGACCTCGCATTGTTCG; pre-rRNA ETS reverse, CGGAGCCAAGTCCCGTGTTCAA; pre-tRNA^{His} forward, CGTGATCGTCTAGTGGTTAG; pre-tRNA^{His} reverse, CCCAACTCCGTGACAATG; pre-tRNA^{Ala} forward, CGCACGGTACTTATAATCAG; pre-tRNA^{Ala} reverse, CCAGGTGAGGCTCGAACTC; pre-tRNA^{Leu} forward, GCGCCAGACTCAAGATTG; pre-tRNA^{Leu} reverse, TGTCAGAAGTGGGATTCG; *Tub* forward, TGGGCCCGTCTGGACCACAA; *Tub* reverse, TCGCCGTCACCGGAGTCCAT; *U3* forward, CACACTAGCTGAAAGCCAAG; *U3* reverse, CGAAGCCCTGCGTCCCGAAC.

Primers used for worms were: *rpc-1* forward, ACGATGGATCACTTGTTTGAAGC; *rpc-1* reverse, GTTCCGACAGTCATTGGGGT; *cdc-42* forward, CTGCTGGACAGGAAGATTACG; *cdc-42* reverse, CTCGGACATTCTCGAATGAAG; *pmp-3* forward, GTTCCCGTGTTCATCACTCAT; *pmp-3* reverse, ACACCGTCGAGAAGCTGTAGA; *Y45F10D.4* forward, GTCGCTTCAAATCAGTTCAGC; *Y45F10D.4* reverse, GTTCTTGTCAAGTGATCCGACA.

For RNA sequencing (RNA-seq) analysis, RNA was further cleaned up with Qiagen RNeasy (Qiagen), ribo-depleted (Ribo-Zero Gold; Illumina) and sequenced on the Illumina platform at Glasgow Polyomics (75 base pairs, pair-end reads). Transcript abundance was estimated with Salmon[42] (https://combine-lab.github.io/salmon/) in quasi-mapping mode onto all *Drosophila* cDNA sequences (BDGP6), imported with tximport (https://bioconductor.org/packages/release/bioc/html/tximport.html) into R (https://www.r-project.org/) and differential expression was determined with DESeq2 (https://bioconductor.org/packages/release/bioc/html/DESeq2.html) using dissection batch as covariate at 10% false discovery rate[43].

Western blots, immunoprecipitation, S2 dsRNA treatment, translation assays and ChIP. Proteins were extracted with trichloroacetic acid from yeast (10 ml culture), S2 cells (0.1–2 ml culture; S2 cells were obtained from L. Partridge, confirmed by growth in appropriate medium and morphology), ten flies or ten dissected mid-guts, washed and resuspended in SDS–PAGE loading buffer, separated by SDS–PAGE and transferred to nitrocellulose. Western blots were

performed with antibodies against puromycin (12D10, Millipore), actin (ab1801 or ab8224, Abcam), Myc (Sigma), Flag (Sigma), phospho-T398-S6K (9209, Cell Signaling), S6K[44] and TOR[21].

Immunoprecipitations were performed on ~2 mg of total protein extracted from 2–5 ml of S2 cell cultures (transfected with pAFW–d*TOR*, treated with dsRNA or untreated) into 50 mM HEPES-KOH pH 8, 100 mM KCl, 5 mM EDTA, 10% glycerol, 0.5% NP-40 and protease inhibitors with 0.5 μl of anti-*d*TOR serum[21], washed five times with the same buffer and eluted into SDS–PAGE sample buffer. The dsRNA against d*TOR* corresponds to a fragment containing bases 3694–4208 of the d*TOR* open reading frame (this is DRSC02811 from DRSC/TRiP) and was generated with the Megascript RNAi Kit (Thermo Fisher Scientific).

Relative translation rates were determined with the SUnSET assay[45]. Ten mid-guts of seven-day-old flies per sample were dissected in ice-cold PBS and kept in 200 μl of ice-cold Schneider's medium followed by incubation in 1 ml of Schneider's medium with 10 μg ml^{-1} puromycin for 30 min at 25 °C. The reaction was stopped by adding 333 μl of 50% trichloroacetic acid. The level of puromycin incorporation was determined by western blot.

ChIP was performed as previously described[46] on chromatin prepared from 7-day-old, wild-type females using anti-TOR antibodies raised against either a recombinant TOR protein fragment[21], or a peptide[22]. The mock control included no antibody. Enrichment after immunoprecipitation was measured relative to input by qPCR. Primers for 5′ and 3′ ends of *aop* and the P2 *InR* promoter have been described previously[46,47]. Other primers used were:

5S rRNA forward, GCCAACGACCATACCACGCTG; 5S rRNA reverse, AGTACT AACCGCGCCCGACG; $tRNA^{Met}$ forward, CGCAGTTGGCAGCGCGTAAG; $tRNA^{Met}$ reverse, CCCCGGGTGAGGCTCGAACT.

pH3, Prospero and anti-HRP staining. Guts from animals at the indicated ages were dissected in ice-cold PBS and immediately fixed in 4% formaldehyde for 30 min. The staining was performed essentially as described[38], with antibodies against phospho-H3 (9701, Cell Signaling), Prospero (Developmental Studies Hybridoma Bank) or horseradish peroxidase[48] (HRP). Guts were mounted in mounting medium with DAPI (Vectastain). The number of pH3-positive cells in each mid-gut was counted under a fluorescence microscope. Representative images were acquired with the Zeiss LSM700 confocal microscope.

Statistical analysis. *Fly and worm data* Survival assays were analysed with the log-rank test in Microsoft Excel, JMP (SAS) or with CPH in R using the survival package (https://cran.r-project.org/web/packages/survival/index.html). All other tests were performed in JMP. Data obtained from dissections, ChIP or western blots were scaled to the dissection, chromatin or replicate batch, except for pH3 counts, to account for batching effects. MANOVA was used to test for the overall effect of RU486 or rapamycin feeding. For ChIP analysis, 'gene' was used as covariate in a linear model with an a priori contrast comparing Pol III- to Pol II-transcribed genes. All regression models had a fully factorial design.

Yeast microfluidics platform The data, including the number of buds produced by each cell and its final event (death or washout), were used for Kaplan–Meier estimation of survival curves with the Lifelines module (Davidson-Pilon, C., Lifelines, (2016), Github repository, https://github.com/CamDavidsonPilon/lifelines) in Python. Plotting and statistical analysis were done in Python.

Code availability. A custom designed code was used to analyse the yeast replicative lifespan data and will be made available upon reasonable request.

Data availability. The data that support the findings of this study are available within the paper and its Supplementary Information files, including source data for figures, or are available from the corresponding author upon reasonable request. RNA-seq data have been deposited in the ArrayExpress database at EMBL-EBI (www.ebi.ac.uk/arrayexpress) under accession number E-MTAB-5252.

28. Verduyn, C., Postma, E., Scheffers, W. A. & Van Dijken, J. P. Effect of benzoic acid on metabolic fluxes in yeasts: a continuous-culture study on the regulation of respiration and alcoholic fermentation. *Yeast* **8,** 501–517 (1992).
29. Lee, S. S., Avalos Vizcarra, I., Huberts, D. H., Lee, L. P. & Heinemann, M. Whole lifespan microscopic observation of budding yeast aging through a microfluidic dissection platform. *Proc. Natl Acad. Sci. USA* **109,** 4916–4920 (2012).
30. Huberts, D. H. *et al.* Construction and use of a microfluidic dissection platform for long-term imaging of cellular processes in budding yeast. *Nat. Protoc.* **8,** 1019–1027 (2013).
31. Papagiannakis, A., de Jonge, J. J., Zhang, Z. & Heinemann, M. Quantitative characterization of the auxin-inducible degron: a guide for dynamic protein depletion in single yeast cells. *Sci. Rep.* **7,** 4704 (2017).
32. Gelino, S. *et al.* Intestinal autophagy improves healthspan and longevity in *C. elegans* during dietary restriction. *PLoS Genet.* **12,** e1006135 (2016).
33. Mathur, D., Bost, A., Driver, I. & Ohlstein, B. A transient niche regulates the specification of *Drosophila* intestinal stem cells. *Science* **327,** 210–213 (2010).
34. Giannakou, M. E. *et al.* Long-lived *Drosophila* with overexpressed *d*FOXO in adult fat body. *Science* **305,** 361 (2004).
35. Niccoli, T. *et al.* Increased glucose transport into neurons rescues Aβ toxicity in *Drosophila*. *Curr. Biol.* **26,** 2291–2300 (2016).
36. Rideout, E. J., Marshall, L. & Grewal, S. S. *Drosophila* RNA polymerase III repressor Maf1 controls body size and developmental timing by modulating $tRNA_i^{Met}$ synthesis and systemic insulin signaling. *Proc. Natl Acad. Sci. USA* **109,** 1139–1144 (2012).
37. Bass, T. M. *et al.* Optimization of dietary restriction protocols in *Drosophila*. *J. Gerontol. A Biol. Sci. Med. Sci.* **62,** 1071–1081 (2007).
38. Alic, N., Hoddinott, M. P., Vinti, G. & Partridge, L. Lifespan extension by increased expression of the *Drosophila* homologue of the IGFBP7 tumour suppressor. *Aging Cell* **10,** 137–147 (2011).
39. Hoogewijs, D., Houthoofd, K., Matthijssens, F., Vandesompele, J. & Vanfleteren, J. R. Selection and validation of a set of reliable reference genes for quantitative sod gene expression analysis in *C. elegans*. *BMC Mol. Biol.* **9,** 10.1186/1471-2199-9-9 (2008).
40. Frendewey, D., Dingermann, T., Cooley, L. & Söll, D. Processing of precursor tRNAs in *Drosophila*. Processing of the 3′ end involves an endonucleolytic cleavage and occurs after 5′ end maturation. *J. Biol. Chem.* **260,** 449–454 (1985).
41. Chan, P. P. & Lowe, T. M. GtRNAdb: a database of transfer RNA genes detected in genomic sequence. *Nucleic Acids Res.* **37,** D93–D97 (2009).
42. Patro, R., Duggal, G., Love, M. I., Irizarry, R. A. & Kingsford, C. Salmon provides fast and bias-aware quantification of transcript expression. *Nat. Methods* **14,** 417–419 (2017).
43. Love, M. I., Huber, W. & Anders, S. Moderated estimation of fold change and dispersion for RNA-seq data with DESeq2. *Genome Biology* **15,** 10.1186/S13059-014-0550-8 (2014).
44. Hahn, K. *et al.* PP2A regulatory subunit PP2A-B′ counteracts S6K phosphorylation. *Cell Metab.* **11,** 438–444 (2010).
45. Schmidt, E. K., Clavarino, G., Ceppi, M. & Pierre, P. SUnSET, a nonradioactive method to monitor protein synthesis. *Nat. Methods* **6,** 275–277 (2009).
46. Alic, N. *et al.* Genome-wide dFOXO targets and topology of the transcriptomic response to stress and insulin signalling. *Mol. Syst. Biol.* **7,** 10.1038/msb.2011.36 (2011).
47. Alic, N. *et al.* Interplay of dFOXO and two ETS-family transcription factors determines lifespan in *Drosophila melanogaster*. *PLoS Genet.* **10,** e1004619 (2014).
48. O'Brien, L. E., Soliman, S. S., Li, X. & Bilder, D. Altered modes of stem cell division drive adaptive intestinal growth. *Cell* **147,** 603–614 (2011).

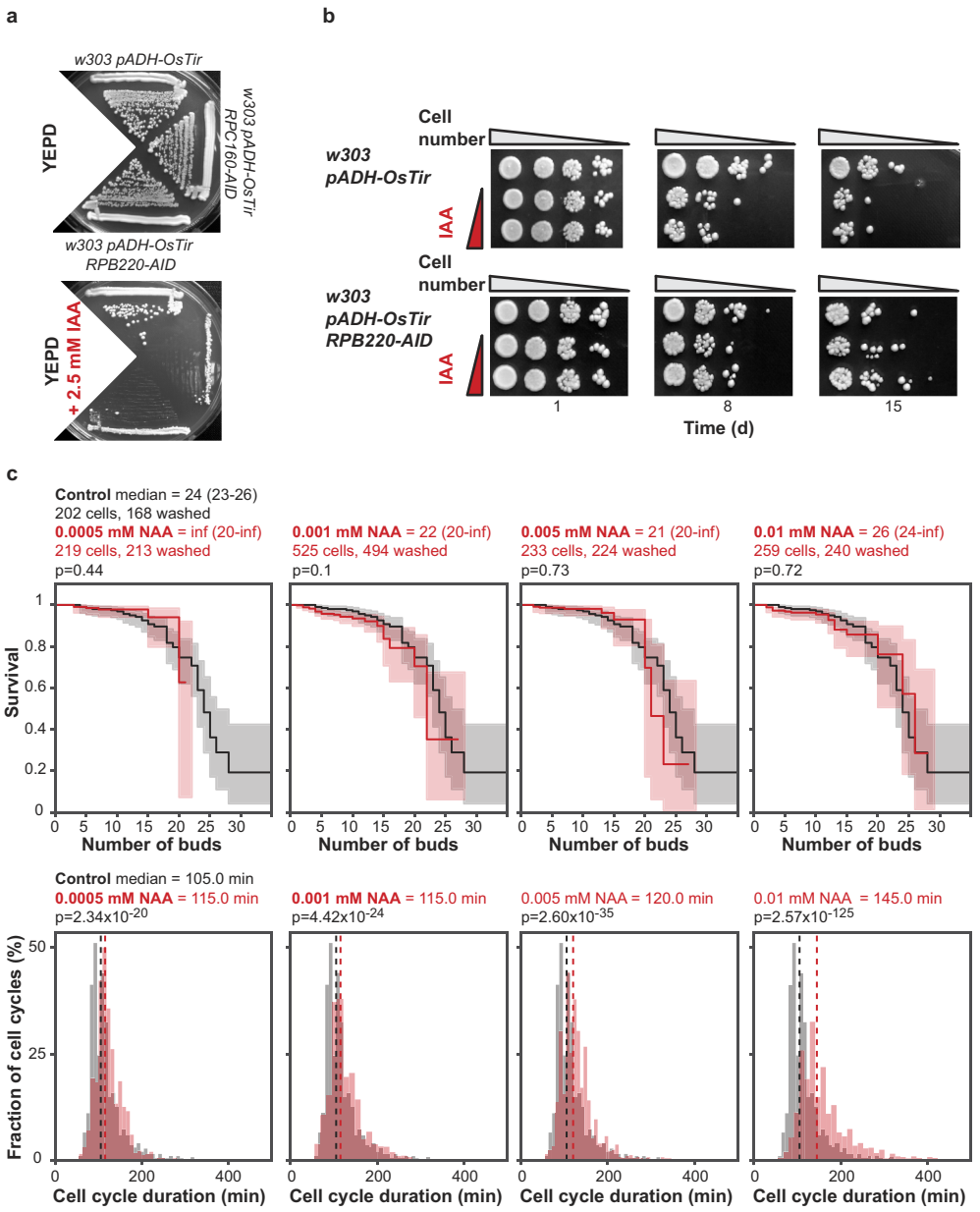

Extended Data Figure 1 | Inhibition of Pol III in yeast. a, The growth of strains carrying *pADH–OsTir* with *RPC160–AID*, *RPB220–AID* or the control lacking an AID fusion in the presence or absence of 2.5 mM IAA (single trial). **b**, Chronological lifespans of the control and *RPB220–AID* strains treated with 0, 0.125 and 0.25 mM IAA. Top panels show a representative of two experiments, performed in parallel with the *RPC160–AID* experiment shown in Fig. 1b. The bottom panels show a single experiment; the improved survival of RPB220–AID was also observed at a higher IAA concentration in a second experiment. **c**, Duration of cell cycle (bottom panels), but not replicative lifespan (top panels), is altered by 1-naphthaleneacetic acid (NAA; analogue of IAA). Both were assessed in the *pADH–OsTir RPC160–AID* strain on a microfluidics dissection platform. The concentrations of NAA span the dynamic range in which the degree of protein depletion can be efficiently modulated in this setup[31]. The same control data are shown in each panel for comparison. One experiment was performed for each NAA concentration. For replicative lifespan experiments, 95% c.i. is indicated by shading (or in brackets for median lifespan), together with log-rank *P* value. A one-sided Mann–Whitney *U* test was used to test for significant differences in cell-cycle duration. No adjustments were made for multiple comparisons. Dashed lines on bottom panels represent medians.

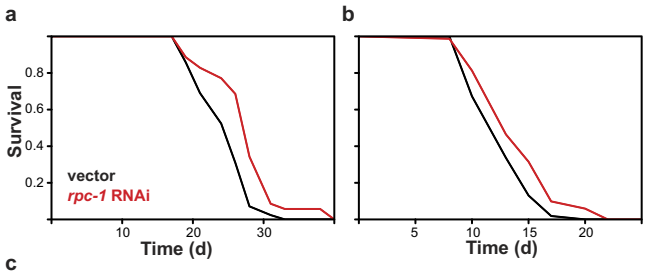

c

Strain	*rpc-1* RNAi	FUDR	Temp	Mean	Dead	Censored	*p*
N2	-	+	25°C	13.01	54	6	
	+	+	25°C	14.31	62	15	0.009
N2	-	+	25°C	14.09	85	42	
	+	+	25°C	15.55	101	42	0.002
N2	-	+	20°C	20.72	59	41	
	+	+	20°C	28.14	22	78	<0.001
N2	-	+	20°C	21.86	48	52	
	+	+	20°C	27.10	29	71	<0.001
N2	-	+	20°C	21.96	52	34	
	+	+	20°C	24.67	21	73	0.032
N2	-	-	20°C	24.71	42	58	
	+	-	20°C	27.77	35	65	<0.001
N2	-	-	20°C	24.67	26	74	
	+	-	20°C	29.43	23	77	0.002
VP303	-	+	20°C	16.89	52	38	
	+	+	20°C	18.92	29	38	0.024
VP303	-	+	20°C	16.36	57	27	
	+	+	20°C	19.06	50	56	<0.001
VP303	-	+	25°C	12.48	78	6	
	+	+	25°C	13.86	97	6	0.009
VP303	-	+	25°C	12.42	79	0	
	+	+	25°C	13.99	80	3	0.001

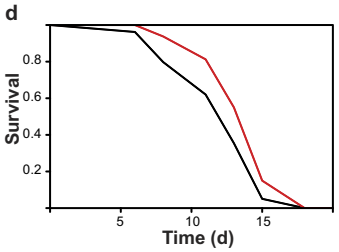

Extended Data Figure 2 | Inhibition of Pol III extends worm lifespan. **a**, Lifespan is extended by feeding N2 worms with *rpc-1* RNAi at 20 °C in the absence of FUDR (log-rank test, $P < 10^{-3}$; control and *rpc-1* RNAi-treated, $n = 100$). **b**, Lifespan is also extended at 25 °C in the presence of FUDR (log-rank test, $P = 9 \times 10^{-3}$; control, $n = 60$; *rpc-1* RNAi, $n = 77$). **c**, Summary of each worm lifespan experiment, including the representative trials presented in the figures. *P* values for log-rank tests are shown. The total number of animals in the trial = dead + censored. In general, fewer worms were censored in control conditions compared to *rpc-1* RNAi conditions (mean number of censored N2 worms at 25 °C = 25% (control) and 38% (*rpc-1* RNAi); mean number of censored N2 worms at 20 °C = 53% (control) and 73% (*rpc-1* RNAi); mean number of censored VP303 at 25 °C = 3% (control) and 4% (*rpc-1* RNAi), and mean number of censored VP303 at 20 °C = 37% (control) and 54% (*rpc-1* RNAi)), which is likely to be due to an increased number of gut explosions in the *rpc-1* RNAi treated worms. 84.9% of censoring events in controls and 85.6% of those in *rpc-1* RNAi-treated animals occurred before the 25th percentile of the survival curve. Overall, increasing the temperature to 25 °C reduced censoring without altering our findings. **d**, Lifespan is extended when the RNAi against *rpc-1* is restricted to the gut by using the VP303 strain at 25 °C in the presence of FUDR (log-rank test, $P = 9 \times 10^{-3}$; control, $n = 84$; *rpc-1* RNAi $n = 103$). In **a**, **b** and **d**, a representative of two trials is shown.

Yeast gene	*Drosophila* orthologue
RPC160 (RPO31)	*CG17209*
RPC128 (RET1)	*RpIII128*
RPC82	*CG12267**
RPC53	*CG5147*
RPC37	*Sin*
RPC34	*CG5380*
RPC31	*CG33051**
RPC25	*CG7339*
RPC17	*Rcp†*
RPC11	*CG33785*

* - identified by homology to the human orthologue
† - low confidence hit identified by homology to the human orthologue

Extended Data Figure 3 | Genes corresponding to unique Pol III subunits in *Drosophila*. The genes encoding the unique Pol III subunits were identified in fruitflies based on their homology to the yeast genes (BLAST, followed by reverse BLAST), or to the human orthologue.

a

Genotype	RU486	Dead	Censored	Median	p
wt	NA	152	0	57	
$dC53^{EY/+}$	NA	143	1	63.5	6.1×10^{-13}
TIGS>dC53^{RNAi}	-	140	3	69.5	
	+	115	24	72.5	3.1×10^{-6}
TIGS>dC160^{RNAi}	-	149	1	71	
	+	155	2	79.5	6.4×10^{-16}
TIGS>dC160^{RNAi}	-	119	2	65	
	+	134	0	70.5	5.9×10^{-7}
TIGS>dC160^{RNAi}	-	140	2	64.5	
	+	152	0	69	1.8×10^{-13}
TIGS>dC160^{RNAi} *males*	-	137	4	57	
	+	137	2	59	0.033
GS5961>dC160^{RNAi}	-	138	1	61.5	
	+	139	3	71	2.3×10^{-4}
GS5961>dC160^{RNAi}	-	113	0	57	
	+	130	0	60.5	1.5×10^{-5}
GS5691>dC160^{RNAi}	-	138	3	64.5	
	+	131	1	68.5	1.0×10^{-3}
TIGS	-	140	1	69.5	
	+	144	1	69.5	0.41
GS5961	-	88	1	68.5	
	+	87	4	68.5	0.88
UAS-dC160^{RNAi}	-	141	1	65	
	+	145	1	65	0.28
*$S_1$106>dC160*^{RNAi}	-	158	0	75.5	
	+	154	1	75.5	0.21
elavGS>dC160^{RNAi}	-	147	1	75.5	
	+	155	0	78	0.026
TIGS>HA-Maf1	-	150	3	63	
	+	142	4	65	0.006

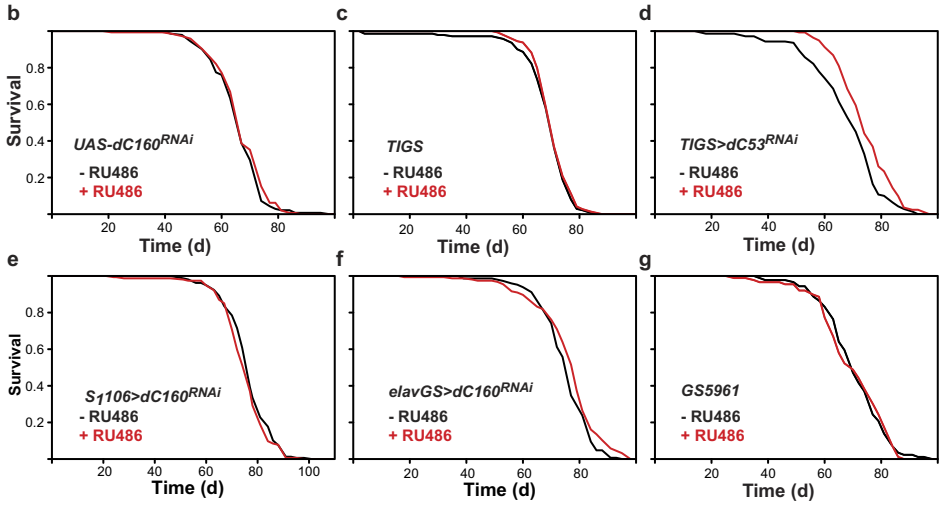

Extended Data Figure 4 | Inhibition of Pol III extends lifespan of flies. **a**, Summary of fly lifespan experiments, including the representative trials presented in the figures, but excluding those with rapamycin (see Extended Data Fig. 8a). Experiments were performed on females unless otherwise noted. The total number of animals in the trial = dead + censored. log-rank test *P* value is reported. **b**, **c**, Feeding with RU486 does not have an effect on the lifespans of: UAS-d$C160^{RNAi}$-only controls (**b**; log-rank test, $P = 0.28$; control, $n = 142$; RU486, $n = 146$); or TIGS-only controls (**c**, log-rank test, $P = 0.41$, control, $n = 141$ RU486, $n = 145$). **d**, Inducing d$C53^{RNAi}$ in the gut by feeding RU486 to female TIGS > d$C53^{RNAi}$ flies extends their lifespan (log-rank test, $P = 3 \times 10^{-6}$; control, $n = 143$; RU486-treated, $n = 139$). **e**, Inducing d$C160^{RNAi}$ predominantly in the fat body by feeding RU486 to $S_1$106 > d$C160^{RNAi}$ flies has no effect on their lifespan (log-rank test, $P = 0.21$; negative control, $n = 158$; RU486, $n = 155$). **f**, Inducing d$C160^{RNAi}$ in neurons by feeding RU486 to elavGS > d$C160^{RNAi}$ females by RU486 has a modest effect on their lifespan ($P = 0.03$, log-rank test; negative control, $n = 148$; RU486, $n = 155$). **g**, RU486 feeding does not have an effect on the lifespan of the GS5961-only controls (log-rank test, $P = 0.88$; negative controls, $n = 89$; RU486, $n = 91$). Experiments in **b**–**g** were performed as single trials.

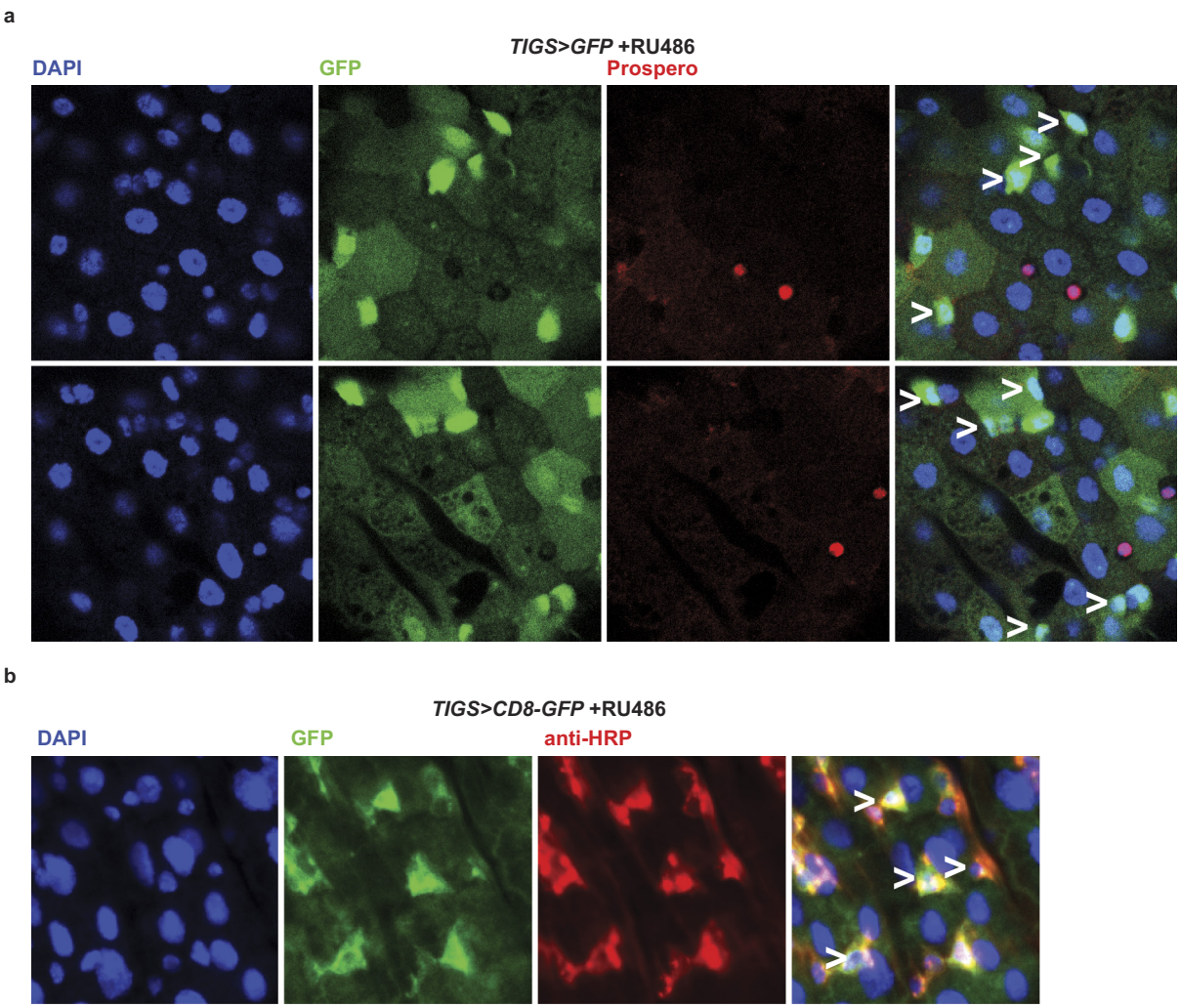

Extended Data Figure 5 | TIGS is active in ISCs. a, **b**, Images from the posterior region of the mid-gut showing GFP expression driven by TIGS in the presence of RU486, and stained with antibodies against Prospero (**a**) and HRP (**b**). GFP is expressed in cells with small nuclei that are negative for Prospero in **a**, and those that are positive for HRP in **b**. Examples of both cell types are indicated with arrows on the merged images. GFP-positive cells can be observed whose morphology and staining pattern correspond closely to those of the ISCs (small nucleus, small cell size, Prospero-negative, HRP-positive; see ref. 48 regarding HRP). TIGS has a complex expression pattern, showing variation between neighbouring cells of the same type and between gut regions. TIGS appears to be active in at least some ISCs. Images are representative of two animals. Images were acquired at 40× (**a**) or 20× (**b**) magnification.

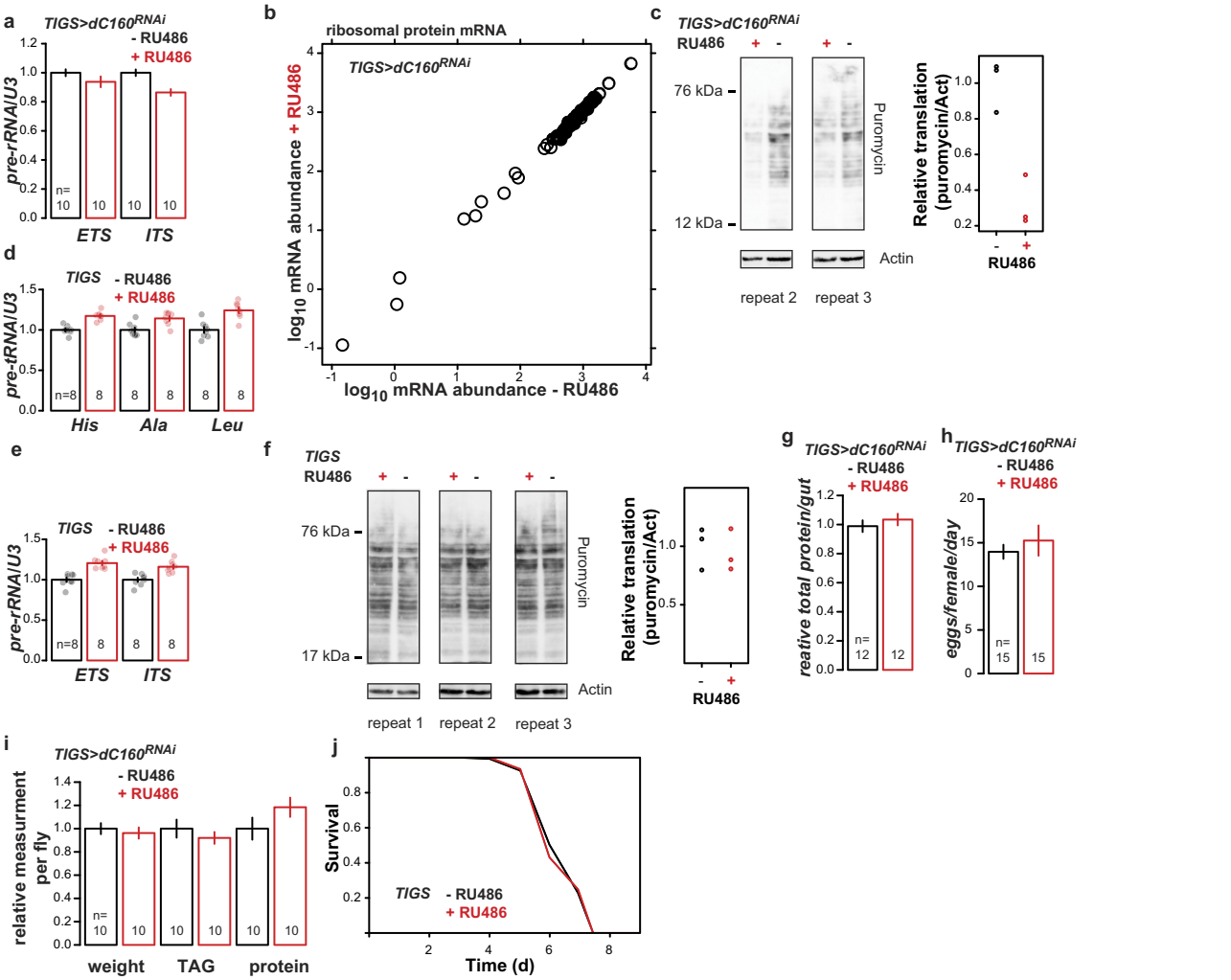

Extended Data Figure 6 | Effects of d*C160*^{RNAi} induction in *Drosophila* adult gut. a–c, Induction of d*C160*^{RNAi} in the gut of TIGS > d*C160*^{RNAi} females results in: decreased levels of 45S pre-rRNA (**a**; MANOVA, $P = 4 \times 10^{-3}$; left to right, c.i. = 0.95–1.1, 0.85–1.0, 0.95–1.1 and 0.81–0.92; EST, 5′ external transcribed spacer; ITS, internal transcribed spacer), indicating a reduction in Pol I activity as a result of Pol III–Pol I crosstalk; unaltered levels of mRNAs encoding ribosomal proteins (**b**; RNA-seq data, no significant differences at 10% false discovery rate; DESeq2, $n = 3$ biologically independent samples), indicating no crosstalk between Pol III and Pol II; decreased protein synthesis (**c**; two further biological repeats and quantification related to Fig. 2e; two-sided *t*-test, $P = 4 \times 10^{-3}$, $n = 3$ biologically independent samples; negative controls, c.i. = 0.65–1.4; RU486, c.i. = −0.033–0.68). **d–f**, Feeding RU486 to female TIGS-only control flies does not result in a significant decreases in: levels of pre-tRNAs (**d**; MANOVA, $P = 1 \times 10^{-4}$; left to right, c.i. = 0.96–1.0, 1.1–1.2, 0.93–1.1, 1.1–1.2, 0.91–1.1 and 1.2–1.3); levels of 45S pre-rRNA (**e**; MANOVA, $P = 2 \times 10^{-4}$; left to right, c.i. = 0.94–1.1, 1.1–1.3, 0.94–1.1 and 1.1–1.2); protein synthesis (**f**; two-sided *t*-test, $P = 0.74$, $n = 3$ biologically independent samples). **g–i**, Induction of d*C160*^{RNAi} in the guts of TIGS > d*C160*^{RNAi} females does not result in significant changes to: total gut protein content (**g**; two-sided *t*-test, $P = 0.43$); female fecundity (**h**; two-sided *t*-test, $P = 0.51$); whole-fly body weight, triacylglycerol or protein content (**i**; two-sided *t*-test, $P = 0.58$, 0.40 or 0.16, respectively). **j**, Feeding RU486 to TIGS-only control females does not result in increased resistance to tunicamycin (log-rank test, $P = 0.89$; negative control, $n = 149$; RU486, $n = 153$; single trial). Bar charts show mean ± s.e.m.; *n*, number of biologically independent samples; overlay, individual data points. Gel source data is shown in Supplementary Fig. 1.

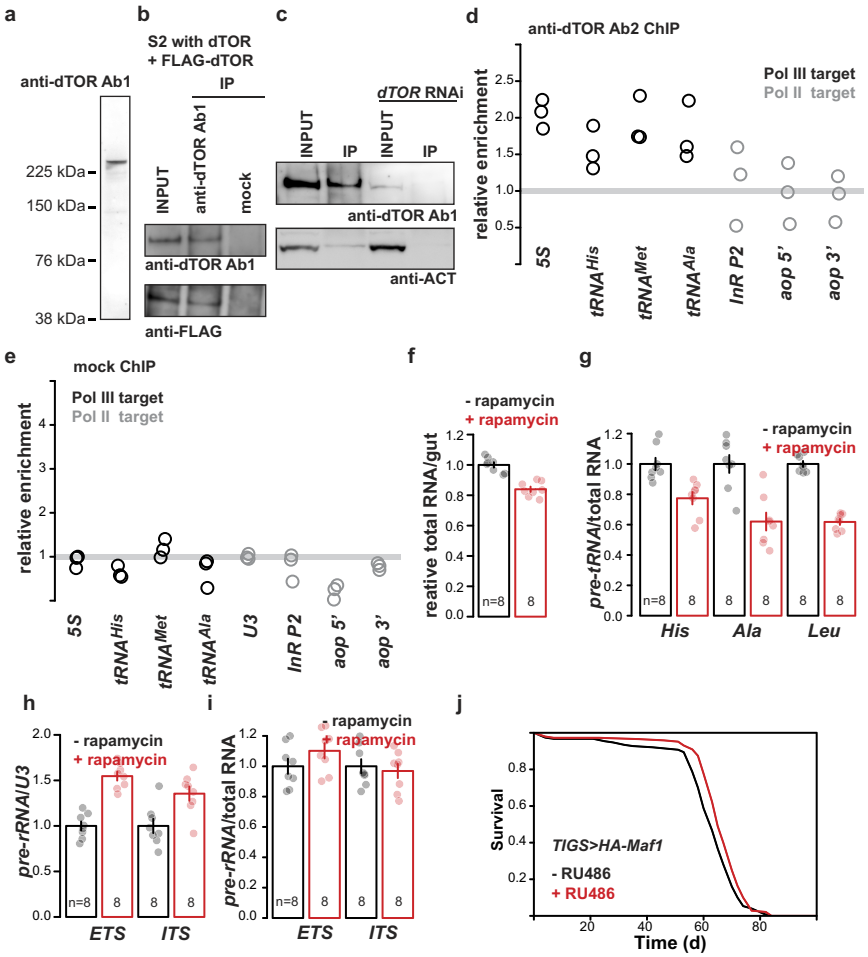

Extended Data Figure 7 | Regulation of Pol III activity by TORC1 in *Drosophila*. **a**, The antibody raised against a recombinant fragment of *Drosophila* TOR protein[21] and used for ChIP (Fig. 3a) recognizes a single band of the expected size on western blots of S2 cell extracts. **b**, The same antibody can immunoprecipitate (IP) TOR from S2 cells expressing endogenous and Flag-tagged TOR. **c**, It can also immunoprecipitate endogenous TOR, and the intensity of this band is reduced upon RNAi treatment against *TOR* in S2 cells with dsRNA. Single experiments were performed for **a**–**c**; the ability of the *TOR* RNAi to reduce the intensity of the band was confirmed in an independent experiment. **d**, ChIP using a different antibody against *Drosophila* TOR (raised against a peptide[22]) shows that relative enrichment of Pol III-transcribed genes is higher than that of Pol II-transcribed genes (linear model with an a priori contrast, $P = 2 \times 10^{-4}$; $n = 3$ biologically independent samples; left to right, c.i. = 1.6–2.6, 0.81–2.3, 1.1–2.7, 0.77–2.8, −0.24–2.5, −0.065–2.0 and 0.13–1.7). **e**, No enrichment of Pol III-transcribed genes over Pol II-transcribed genes is observed after mock ChIP with no antibody (linear model with an a priori contrast, $P = 0.09$, $n = 3$ biologically independent samples). **f**, Rapamycin feeding results in a decrease in total RNA content of the adult gut (two-sided *t*-test, $P < 10^{-4}$). **g**, Rapamycin feeding results in reduction of pre-tRNAs relative to total RNA in the fly gut (MANOVA, $P = 10^{-4}$). **h**, **i**, Rapamycin feeding does not result in a reduction of pre-rRNA in the fly gut relative to *U3* (**h**; MANOVA, $P < 10^{-4}$) or total RNA (**i**; MANOVA, $P = 0.57$). **j**, *HA–Maf1* induction specifically in the gut by feeding RU486 to female TIGS > HA–*Maf1* flies extends their lifespan (log-rank test, $P = 0.006$; control, $n = 153$; RU486, $n = 146$; single trial). Bar charts show mean ± s.e.m.; *n*, number of biologically independent samples; overlay, individual data points. Gel source data is shown in Supplementary Fig. 1.

a

Summary

Genotype	RU486	Rapamycin	Dead	Censored	Median	p
TIGS>dC160^{RNAi}	-	-	134	1	69	
	+	-	144	0	78	6.2×10^{-15}
	-	+	140	1	75.5	2.7×10^{-13}
	+	+	144	2	78	2.1×10^{-18}
TIGS>dC53^{RNAi}	-	-	121	14	72	
	+	-	117	18	77	1.7×10^{-5}
	-	+	116	4	77	5.9×10^{-12}
	+	+	124	13	77	5.1×10^{-6}
GS5961>dC160^{RNAi}	-	-	113	0	57	
	+	-	130	0	60.5	1.5×10^{-5}
	-	+	145	0	65	3.9×10^{-12}
	+	+	144	0	60.5	6.4×10^{-9}

Cox Proportional Hazards analyses

Genotype	Effect	Coef.	Exp(coef)	SE(coef)	z	p
TIGS>dC160^{RNAi}	RU486	-1.2	0.30	0.13	-9.1	$<2\times10^{-16}$
	Rapamycin	-0.98	0.37	0.13	-7.6	2.2×10^{-14}
	interaction	1.02	2.8	0.18	5.8	7.5×10^{-9}
TIGS>dC53^{RNAi}	RU486	-0.56	0.57	0.13	-4.3	2.1×10^{-5}
	Rapamycin	-1.01	0.37	0.14	-7.3	2.3×10^{-13}
	interaction	0.97	2.6	0.19	5.2	2.5×10^{-7}
GS5961>dC160^{RNAi}	RU486	-0.56	0.57	0.13	-4.3	1.7×10^{-5}
	Rapamycin	-0.97	0.38	0.13	-7.5	8.1×10^{-14}
	interaction	0.91	2.5	0.18	5.1	2.8×10^{-7}

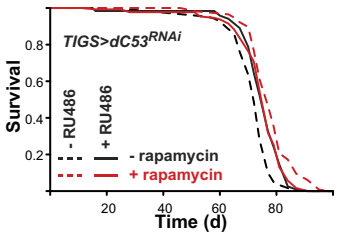

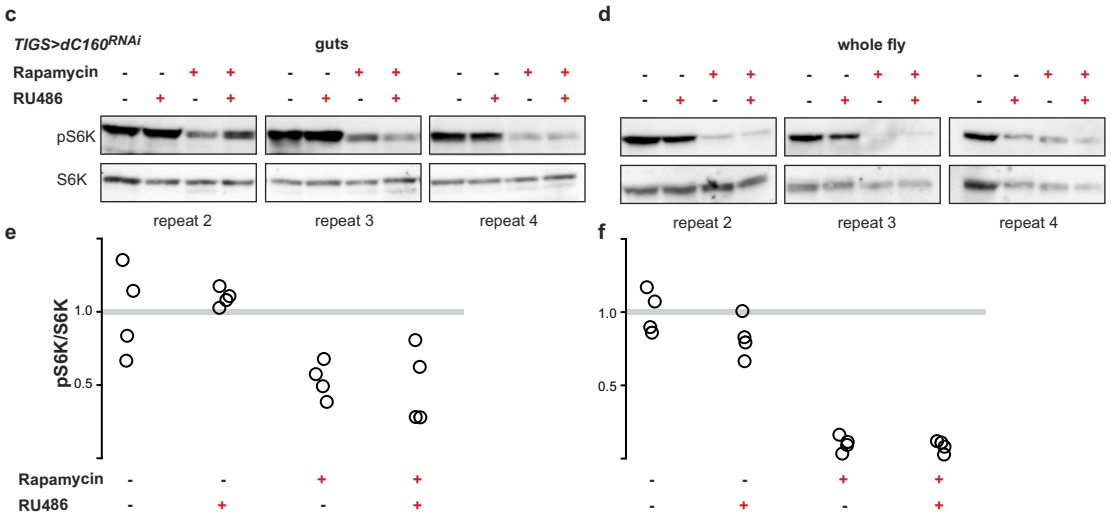

Extended Data Figure 8 | Relationship between TORC1 and Pol III. **a**, Summary of fly lifespan experiments examining the epistasis between Pol III and TORC1 inhibition (top), including the results of CPH analyses (bottom). The summary (top) shows log-rank test *P* values, relative to the no-RU486, no-rapamycin control, and the total number of animals in the trial = dead + censored. **b**, Induction of d*C53^{RNAi}* in the adult gut by feeding RU486 to female TIGS > d*C53^{RNAi}* flies, and rapamycin feeding both extend lifespan and their effects are not additive (for statistical analysis see **a**; control, $n = 135$; RU486, $n = 135$; rapamycin, $n = 120$; rapamycin + RU486, $n = 137$; single trial). **c**–**f**, Rapamycin, but not induction of d*C160^{RNAi}* in the gut of female TIGS > d*C160^{RNAi}* flies with RU486, reduces phosphorylation of S6K in the gut (linear model; rapamycin, $P = 3 \times 10^{-4}$; RU486, $P = 0.77$; interaction, $P = 0.55$; left to right, c.i. = 0.51–1.5, 1.0–1.2, 0.33–0.73 and 0.08–0.91) and whole flies (linear model; rapamycin, $P < 10^{-4}$; RU486, $P = 0.10$; interaction, $P = 0.16$; left to right, c.i. = 0.77–1.2, 0.60–1.0, 0.016–0.19 and 0.019–0.15). Additional biological repeats related to Fig. 3g are presented for the gut (**c**) and the whole fly (**d**). These are quantified in **e** and **f**, respectively. **c**–**f** show data from four biologically independent samples. Gel source data are shown in Supplementary Fig. 1.

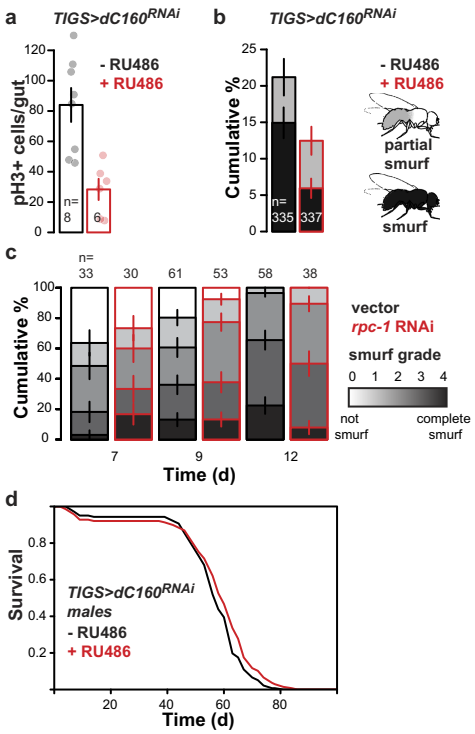

Extended Data Figure 9 | Inhibition of Pol III in the gut preserves organ health. a, Induction of d*C160*^{RNAi} in the gut by feeding RU486 to female adult TIGS > d*C160*^{RNAi} flies suppresses accumulation of pH3-positive cells in old flies (two-tailed *t*-test, $P = 1 \times 10^{-3}$; control, c.i. = 58–110; RU486, c.i. = 10–46). **b**, Induction of d*C160*^{RNAi} in the gut by feeding RU486 to adult female TIGS > d*C160*^{RNAi} flies suppresses loss of gut barrier function (number of Smurfs) in old flies (χ^2-test, $P = 5 \times 10^{-4}$; control, c.i. = 16–26%; RU486, c.i. = 8.7–16%, percentage of Smurfs). **c**, *rpc-1* RNAi suppresses the severity of the age-related loss of gut barrier function in worms (OLR; effect of age, $P < 10^{-4}$; *rpc-1* RNAi, $P = 0.51$; interaction, $P = 0.01$; left to right, c.i. = 5.0–31%, 16–50%, 24–48%, 25–51%, 53–78% and 34–66%, percentage of Smurf grades 3 and 4). Age-related loss of gut barrier function in worms has been described previously[32]. **d**, Induction of d*C160*^{RNAi} in the gut by feeding RU486 to adult male TIGS > d*C160*^{RNAi} flies results in a small but significant extension of lifespan (log-rank test, $P = 0.03$; no-RU486, $n = 141$; RU486, $n = 139$; single trial). Bar charts show mean ± s.e.m.; *n*, number of animals; overlay, individual data points.

nature research

Corresponding author(s): Nazif Alic, Jennifer M.A. Tullet

☐ Initial submission ☐ Revised version ☒ Final submission

Life Sciences Reporting Summary

Nature Research wishes to improve the reproducibility of the work that we publish. This form is intended for publication with all accepted life science papers and provides structure for consistency and transparency in reporting. Every life science submission will use this form; some list items might not apply to an individual manuscript, but all fields must be completed for clarity.

For further information on the points included in this form, see Reporting Life Sciences Research. For further information on Nature Research policies, including our data availability policy, see Authors & Referees and the Editorial Policy Checklist.

Experimental design

1. Sample size

   Describe how sample size was determined.

   Sample sizes were based on previous experiments of the same type.

2. Data exclusions

   Describe any data exclusions.

   Some (very few) data points were excluded due to technical failure/issues.

3. Replication

   Describe whether the experimental findings were reliably reproduced.

   There were no attempts at replication that failed.

4. Randomization

   Describe how samples/organisms/participants were allocated into experimental groups.

   The samples were allocated to groups randomly, in a way so as to protect against or reduce any batching effects.

5. Blinding

   Describe whether the investigators were blinded to group allocation during data collection and/or analysis.

   The investigators were not blinded to group allocations.

   Note: all studies involving animals and/or human research participants must disclose whether blinding and randomization were used.

6. Statistical parameters

   For all figures and tables that use statistical methods, confirm that the following items are present in relevant figure legends (or in the Methods section if additional space is needed).

n/a	Confirmed
☐	☒ The exact sample size (*n*) for each experimental group/condition, given as a discrete number and unit of measurement (animals, litters, cultures, etc.)
☐	☒ A description of how samples were collected, noting whether measurements were taken from distinct samples or whether the same sample was measured repeatedly
☐	☒ A statement indicating how many times each experiment was replicated
☐	☒ The statistical test(s) used and whether they are one- or two-sided (note: only common tests should be described solely by name; more complex techniques should be described in the Methods section)
☐	☒ A description of any assumptions or corrections, such as an adjustment for multiple comparisons
☐	☒ The test results (e.g. *P* values) given as exact values whenever possible and with confidence intervals noted
☐	☒ A clear description of statistics including central tendency (e.g. median, mean) and variation (e.g. standard deviation, interquartile range)
☐	☒ Clearly defined error bars

See the web collection on statistics for biologists for further resources and guidance.

Software

Policy information about availability of computer code

7. Software

Describe the software used to analyze the data in this study.	JMP 13 (and 10, 11 and 12), R 3.4.0 (and below), Excel 15.29 (and below), Python 2.7, Salmon 0.7.2 OSX 10.11, ImageJ 1.51 (and below).

For manuscripts utilizing custom algorithms or software that are central to the paper but not yet described in the published literature, software must be made available to editors and reviewers upon request. We strongly encourage code deposition in a community repository (e.g. GitHub). *Nature Methods* guidance for providing algorithms and software for publication provides further information on this topic.

Materials and reagents

Policy information about availability of materials

8. Materials availability

Indicate whether there are restrictions on availability of unique materials or if these materials are only available for distribution by a for-profit company.	There are no restrictions on availability of unique materials generated and used in the study.

9. Antibodies

Describe the antibodies used and how they were validated for use in the system under study (i.e. assay and species).	Rabbit polyclonal anti-Actin from Abcam (ab1801); validated by the supplier, correct size on western blots. Mouse anti-Actin from Abcam (ab8224); validated by the supplier, correct size on western blots. Mouse monoclonal anti-Puromycin from Millipore (MABE343); clone recommended for this method (12D10). Mouse monoclonal anti-Prospero from Developmental Studies Hybridoma Bank (MR1A); widely used clone. Mouse monoclonal anti-myc from Sigma (M4439); widely used clone (9E10). Polyclonal anti-dTOR antibodies were provided by G. Juhasz and A. Teleman; published and cross-validated for ChIP. The one from G. Juhasz was confirmed by western, IP and RNAi against dTOR. Purified, polyclonal rabbit anti-HRP from Jackson Immunoresearch (323-025-021); validated for IF by the supplier. Rabbit polyclonal anti-phosphoS6 from Cell Signaling (9209); validated by the supplier and widely used. Anti-total S6 was provided by A. Teleman; previously published use for western blots, band of correct size.

10. Eukaryotic cell lines

a. State the source of each eukaryotic cell line used.	The parental yeast line was obtained from C. Bouchoux and F. Uhlmann. S2 cells were obtained from L. Partridge.
b. Describe the method of cell line authentication used.	Confirmed by growth in specific media and morphology.
c. Report whether the cell lines were tested for mycoplasma contamination.	We didn't use any cell lines that could have mycoplasma contamination. We only used Drosophila cells or yeast.
d. If any of the cell lines used are listed in the database of commonly misidentified cell lines maintained by ICLAC, provide a scientific rationale for their use.	No cell lines used are in the database of commonly misidentified cell lines.

Animals and human research participants

Policy information about studies involving animals; when reporting animal research, follow the ARRIVE guidelines

11. Description of research animals

Provide details on animals and/or animal-derived materials used in the study.	We used: (1) Caenorhabditis elegans, adult hermaphrodites, N2 or VP303 strains; (2) Drosophila melanogaster, wild-type Dahomey stock with w1118 mutation and TIGS (a.k.a. TIGS-2), GS5961, S1106, elavGS, UAS-HA-Maf1, UAS-dC160RNAi and UAS-dC53RNAi (v30512 and v103810 from Vienna Drosophila Resource Centre), and dC53EY22749 (CG5147EY22749 from Bloomington Stock Centre) in the same background, adult females and males, as indicated. These are not protected animal species. No other animal species were used.

Policy information about studies involving human research participants

12. Description of human research participants

Describe the covariate-relevant population characteristics of the human research participants.	N/A